

The Classical Wave Equation: A Guide to Theoretical Concepts for Enhanced Student Understanding

Abstract. This paper serves as an intuitive guide for students' understanding of the one dimensional classical wave equation. The focus aimed at bridging the gap between theoretical derivations and its practical applications, with a particular emphasis on modeling the elastic properties of structures. We first introduced the foundational principles and theoretical derivation and extend into the application of Fourier series techniques to unravel deep concepts not explained in engineering mathematical textbooks that students find difficult to comprehend. We emphasise that theoretical foundations are not abstract phenomena but serve as the building blocks of engineering principles and design. In this regard, we applied analytical and numerical methods to reinforce critical concepts that would have otherwise remained abstract outside the realm of demonstration and practical application. The numerical aspect aids with understanding the theory as it showed the evolution of wave patterns, which agreed with the analytical solution. The results obtained from comparing both analytical and numerical solutions show that different time step values (Δt) influenced the numerical solutions only by shifting the function, $f(x)$, in amplitude, but its shape and agreement with the analytical solution were maintained. This research demonstrates how innovative teaching techniques, which include the combined use of analytical and numerical methods, can be applied to improve students' understanding of mathematical theory and physical applications in engineering.

Keywords: Wave equation, Engineering Mathematics, Fourier series, Numerical Analysis, structural dynamics.

1 Introduction

Engineering mathematics is the cornerstone of various engineering disciplines, forming the bedrock upon which practical applications are built. One such foundation is the classical wave equation, which is a fundamental model that plays a pivotal role of our understanding on wave propagation and vibrations. Within the context of engineering education, the wave equation serves as an integral component on Partial Differential Equations (PDEs) and Vector Calculus coursework. However, students frequently encounter difficulties in understanding its theoretical origins and practical implications.

In addressing this issue, this paper was geared towards enhancing students' grasp of the theoretical aspects of the classical wave equation and its interplay with real-world applications. We achieved this by synthesizing the complete analytical solution with numerical methods while reviewing recent research that contributes to the broader understanding of the mathematical concepts. For instance, a current shift in teaching differential equations (DEs) require visual interpretation of the solution space. This emphasises the need to adapt an analytical solution into a numerical form for enhanced student understanding. In response to the lack of studies on this approach Rezvanifard et al. (2023) designed two collaborative tasks (sophism and paradox) for undergraduate engineering students. These tasks aimed to investigate students' understanding of exact DEs and to analyse their learning processes within small groups, which involved 135 undergraduate students. The findings highlight that engaged graphical-based learning facilitated a more conceptual grasp of the subject among students.

In a research conducted by Ye, et al. (2023), it was found that effective learning in both computational thinking (CT) and mathematics was fostered by the adoption of geometrised programming and student-centered instructional methods. Their work revealed that CT-based mathematics learning involves a dynamic and cyclical cognitive process that intertwines mathematical reasoning and computational thinking. This process, as argued, unfolds through three key facets: 1. Students utilise mathematical principles as they engage in the creation of CT artifacts. 2. These principles play a pivotal role in the anticipation and interpretation of CT-generated outputs. It serves as a lens through which students can make sense of CT results within a mathematical framework. 3. An interesting finding was that students simultaneously develop new mathematical insights while engaging in CT activities. This parallel evolution of understanding is testament to the interconnectedness of theory and numerical methods on students' learning outcomes. It underscores the dynamic and mutually reinforcing relationship between mathematical theory and visual interpretation, shedding light on the coupled nature of their interaction.

With respect to the wave equation, Yang et al. (2023) presented an investigation on even entire functions of order one as solutions to the classical wave equation in a one-dimensional (1D) space. They propose a conjecture suggesting that these functions have purely real zeros throughout the complex plane, offering an intriguing connection between number theory and wave equations. Wang et al. (2022) introduced a fast guided wave imaging method based on convolutional neural networks (CNN) for corrosion mapping. This method allows for real-time prediction of corrosion damage thickness using guided wave data, which demonstrated high accuracy and resistance to noise. Walker et al. (2023) developed VisualPDE as an online interactive solver for 1D and 2D partial differential equation (PDE) systems. VisualPDE enables instantaneous and interactive exploration of complex nonlinear systems, making it valuable for

education, research, and knowledge exchange in mathematical biology and related fields. Nagarajiah (2021) proposed the Simultaneous Basis Function Approximation and Parameter Estimation (SNAPE) technique, which employs measured spatiotemporal responses to infer the governing PDEs. SNAPE demonstrates robust parameter estimation for PDEs, even in the presence of high noise levels, with applications ranging from Schrödinger equations to Navier-Stokes equations.

Ding et al. (2022) investigated the use of space-time fractional-order operators in simulating linear elastic waves in 1D periodic structures on viscoelastic foundations. They develop a homogenised model that is capable of capturing both material and geometric inhomogeneity and viscoelastic behavior. This method offered new insights into modeling wave dynamics and frequency band gaps. Chen et al. (2022) proposed a physics-guided machine learning-based inverse design method for multifunctional wave control in active metabeams. The approach combined machine learning with the transfer matrix method, providing a versatile means to design metamaterials with desired physical responses. Prieur et al. (2014) studied a nonlinear 1D wave equation describing string deflection with distributed actuation subject to saturation. They establish well-posedness and asymptotic stability using nonlinear semigroups and Lyapunov techniques to showcase the importance of sector conditions in describing the saturating input. Lomovtsev et al. (2021) used a modified method of characteristics to derive explicit solutions for a linear mixed problem in a general 1D wave equation with time-varying characteristic second derivatives in boundary conditions. Their work provides criteria for the well-posedness of the problem and emphasises data smoothness and consistency conditions. Guo et al. (2018) addressed the error feedback regulator problem for the 1D wave equation with harmonic disturbance. They propose an adaptive control approach that achieves tracking error regulation and state boundedness by utilising measured tracking error and disturbance parameter estimation.

In our case, we aimed to simplify the theoretical foundations of the classical wave equation by offering clear, step-by-step explanations for engineering students at the undergraduate level. To address the practical context of our work, we relate the wave equation to a real-world scenario by characterising the elastic properties of a beam structure as an elastic string. Once the relationship of our objective was established, we then converted the analytical solution to a numerical form in an effort to bridge theory and application. This served as a prerequisite and motivation for additional coursework on the discretisation of PDEs, where numerical methods are taught, to demonstrate that theoretical concepts in engineering is not an abstract phenomenon but serves as the bedrock of all engineering principles and design. Our contributions can be summarised as follows:

1. We have provided clear explanations of the theoretical foundations of the classical 1D wave equation. Our aim was to make this complex concept more approachable for undergraduate engineering students.
2. To facilitate learning, we have offered a detailed, step-by-step derivation to help students grasp the complete mathematical underpinnings.
3. We have explored segments of the classical wave equation, which are not extensively covered in standard textbooks such as the integration by parts and the use of orthogonality of functions as a Fourier series technique. This provide students with a deeper understanding of the fundamental concept.

4. To bridge theory and real-world scenarios, we have taken the theoretical wave equation and related it to a practical context by modeling the elastic properties of a beam as a 1D string. This helped students see the relevance and applicability of theoretical concepts. For simplicity, we used derivations and variable names inline with Stroud and Booth (2007) advanced engineering mathematics for consistency.

1.1 The Wave Equation: A Theoretical Overview

To solve the wave equation, we often need to specify boundary conditions and initial conditions. The boundary conditions, given at $x = 0$ and $x = L$ in a one dimensional (1D) model is applied to help determine the first two arbitrary constants in the general solution. These conditions could be, for example, fixed ends ($u(0, t) = 0$ and $u(L, t) = 0$) or free ends ($\frac{\partial u}{\partial x}(0, t) = 0$ and $\frac{\partial u}{\partial x}(L, t) = 0$).

However, to fully solve the complete wave equation, we also need to consider the initial conditions. These conditions specify the initial displacement, $u(x, 0)$, and the initial velocity, $\frac{\partial u}{\partial t}(x, 0)$, of the wave at $t = 0$. The wave equation is given by:

$$\frac{\partial^2 u}{\partial t^2} = c^2 \frac{\partial^2 u}{\partial x^2} \quad (1)$$

To solve (1), we aim to find a solution u that is not identically zero, satisfying boundary conditions, with the property that the dependence of u on x and t is separated. We assume a solution of the form $u(x, t) = X(x)T(t)$, where X is a function of x only, and T is a function of t only, such that the equivalent of each separable term equals a constant k . Separating variables, we obtain:

$$X'' = kX \quad (2)$$

$$T'' = c^2 kT \quad (3)$$

To obtain a solution we seek a value, k , that satisfies the physical system.

1. If $k = 0$:

From (2), we have $X'' = 0$, leading to $X = ax + b$. However, $X = 0$ at $x = 0$ and $x = l$, implying $a = 0$ and $b = 0$, resulting in $X = 0$, which is not oscillatory as required.

2. If k is positive, let $k = p^2$:

From (2), we have $X'' - p^2 X = 0$, leading to the auxiliary equation $m^2 - p^2 = 0$. Solving this gives $m = \pm p$. Thus, the solution for X is:

$$X = Ae^{px} + Be^{-px}$$

However, $X = 0$ at $x = 0$ and $x = l$, implying $A = B = 0$, resulting in $X = 0$, which is not oscillatory as required.

3. If k is negative, let $k = -p^2$:

From (2) and (3), we have $X'' + p^2 X = 0$ and $T'' + c^2 p^2 T = 0$, leading to the following solutions that fit the requirements for an oscillatory function:

$$X = A \cos(px) + B \sin(px), \quad T = C \cos(cpt) + D \sin(cpt)$$

Combining the spatial and temporal solutions, we get:

$$u(x, t) = XT = (A \cos(px) + B \sin(px))(C \cos(cpt) + D \sin(cpt))$$

If we set $cp = \lambda$, we can simplify this further:

$$u(x, t) = (A \cos(px) + B \sin(px))(C \cos(\lambda t) + D \sin(\lambda t))$$

where A, B, C , and D are arbitrary constants we need to find.

Now, we considered the boundary conditions:

(a) $u = 0$ when $x = 0$ for all values of t . This implies $A = 0$.

(b) $u = 0$ when $x = l$ for all values of t . This implies $\sin(pl) = 0$ and we know that $\sin(n\pi) = 0$, so that $pl = n\pi$, which gives us $p_n = \frac{n\pi}{l}$ for $n = 1, 2, 3, \dots$. So, the final solution is:

$$u(x, t) = B_n \sin\left(\frac{n\pi x}{l}\right) (C \cos(\lambda t) + D \sin(\lambda t))$$

where n is an integer, $p_n = \frac{n\pi}{l}$, and B_n is determined by the initial condition and Fourier techniques. This solution can be generalised as follows:

$$u(x, t) = \sum_{n=1}^{\infty} \sin\left(\frac{n\pi x}{l}\right) (C_n \cos(\lambda t) + D_n \sin(\lambda t)) \quad (4)$$

Now, we need to determine the coefficients C_n and D_n by applying initial conditions:

(c) At $t = 0$, $u(x, 0) = f(x)$ for $0 \leq x \leq l$. Therefore, from our general solution for $n = 1, 2, 3, \dots, r$, we have:

$$f(x) = \sum_{n=1}^r \sin\left(\frac{n\pi x}{l}\right) (C_n \cos(\lambda t) + D_n \sin(\lambda t)) \quad (5)$$

At $t = 0$, when $\cos(0) = 1$ and $\sin(0) = 0$, the equation simplifies to:

$$f(x) = \sum_{n=1}^r \sin\left(\frac{n\pi x}{l}\right) C_n \quad (6)$$

(d) Also at $t = 0$, $\frac{\partial u}{\partial t}(x, 0) = g(x)$ for $0 \leq x \leq l$. We differentiate our general solution with respect to t and set $t = 0$, which yields:

$$\frac{\partial u}{\partial t} = \sum_{r=1}^r \left(\frac{c\pi}{l} r \sin\left(\frac{r\pi x}{l}\right) D_r \cos(\lambda t) - \frac{c\pi}{l} r \sin\left(\frac{r\pi x}{l}\right) C_r \sin(\lambda t) \right) \quad (7)$$

Now, applying $\frac{\partial u}{\partial t}(x, 0) = g(x)$ at $t = 0$, we have:

$$g(x) = \sum_{r=1}^r \frac{c\pi}{l} r \sin\left(\frac{r\pi x}{l}\right) D_r \quad (8)$$

With initial boundary conditions satisfied, we proceed to determine the coefficients C_r and D_r from equations (6) and (8) using Fourier series and the orthogonality of functions.

Derivation of Fourier Sine Series Coefficients

We want to find the coefficients C_r and D_r that make $u(x, 0)$ and $\frac{\partial u}{\partial t}(x, 0)$, the Fourier sine series of $f(x)$ and $g(x)$ respectively, given by:

$$u(x, 0) = \sum_{r=1}^{\infty} C_r \sin\left(\frac{r\pi x}{L}\right) = f(x) \quad (9)$$

and

$$u(x, 0) = \frac{c\pi}{L} \sum_{r=1}^{\infty} D_r r \sin\left(\frac{r\pi x}{L}\right) = g(x) \quad (10)$$

The result we wish to obtain are as follows:

$$C_r = \frac{2}{L} \int_0^L f(x) \sin\frac{r\pi x}{L} dx \quad r = 1, 2, 3, \dots \quad (11)$$

and

$$D_r = \frac{2}{rc\pi} \int_0^L g(x) \sin\frac{r\pi x}{L} dx \quad r = 1, 2, 3, \dots \quad (12)$$

To determine coefficients C_r and D_r in equations (11) and (12), in relation to (9) and (10), we use the orthogonality property of Fourier series. First, we multiply both sides of (9) by $\sin\left(\frac{m\pi x}{L}\right)$ and integrate over the interval $[0, L]$:

$$\int_0^L C_r \sin\left(\frac{n\pi x}{L}\right) \left[\sin\left(\frac{m\pi x}{L}\right)\right] dx = \int_0^L f(x) \left[\sin\left(\frac{m\pi x}{L}\right)\right] dx \quad (13)$$

Using the orthogonality property of sine functions, all terms except the one with $n = m$ (corresponding to the same eigenvalue) will integrate to zero.

Note: The orthogonality property of sine functions states that the sine functions are orthogonal (perpendicular) to each other over certain intervals (Stroud and Booth, 2007). Specifically, for two distinct positive integers m and n , the following property holds:

$$\int_0^L \sin\left(\frac{n\pi x}{L}\right) \sin\left(\frac{m\pi x}{L}\right) dx = \begin{cases} 0 & \text{if } m \neq n \\ \frac{L}{2} & \text{if } m = n \end{cases} \quad (14)$$

This property implies that when two different sine functions are multiplied and integrated over a certain interval, the result is zero, indicating their orthogonality. However, when the two sine functions have the same frequency (i.e., when $m = n$), the integral evaluates to $\frac{L}{2}$. Hence, from equation (13), w.r.t (14), we have:

$$\int_0^L C_r \sin^2\left(\frac{m\pi x}{L}\right) dx = \int_0^L f(x) \sin\left(\frac{m\pi x}{L}\right) dx \quad (15)$$

On the **LHS**, after solving the integral, (see **Appendix** for derivation). we see:

$$\int_0^L C_r \sin^2\left(\frac{m\pi x}{L}\right) dx = \frac{L}{2} B_m \quad (16)$$

on the **RHS**, we have:

$$\int_0^L f(x) \sin\left(\frac{m\pi x}{L}\right) dx \quad (17)$$

Therefore, by combining (16) and (17), equation (15), becomes:

$$\frac{L}{2}C_r = \int_0^L f(x) \sin\left(\frac{m\pi x}{L}\right) dx \quad (18)$$

To find the coefficient C_r , we divide both sides by $\frac{L}{2}$ or multiply by its conjugate, $\frac{2}{L}$, to obtain:

$$C_r = \frac{2}{L} \int_0^L f(x) \sin\left(\frac{m\pi x}{L}\right) dx \quad (19)$$

This equation provides the formula to calculate the coefficients C_r based on the given initial displacement function $f(x)$ over the length of the interval L .

We have shown how Fourier series can be used to find the two arbitrary constants C_r and D_r as the final solution, in (20), for the Wave equation.

$$u(x, t) = \sum_{r=1}^{\infty} \sin \frac{r\pi a}{L} \left(\left[\frac{2}{L} \int_0^L f(a) \sin \frac{r\pi a}{L} da \right] \cos \frac{rc\pi t}{L} + \left[\frac{2}{rc\pi} \int_0^L g(a) \sin \frac{r\pi a}{L} da \right] \sin \frac{rc\pi t}{L} \right) \quad (20)$$

Note, $f(a)$ and $g(a)$ are used as initial conditions in the final result. The variable of integration (a) is now used instead of x to avoid confusion with (x) in $u(x, t)$.

2 Wave Propagation in a 1D Steel Beam

We wish to model a beam as a 1D string to understand its elastic properties and wave propagation behaviour as an application of the theoretical foundation. Consider a 1D steel beam with a length of 20 cm subjected to the following conditions as illustrated in Figure 1 and equations (21-24).

$$u(0, t) = 0 \quad (\text{fixed end point at } x = 0) \quad (21)$$

$$u(20, t) = 0 \quad (\text{fixed end point at } x = 20) \quad (22)$$

$$u(x, 0) = f(x) \quad (\text{initial vertical displacement profile}) \quad (23)$$

$$\frac{\partial u}{\partial t}(x, 0) = 0 \quad (\text{zero initial velocity}) \quad (24)$$

The initial displacement profile $f(x)$ due to an imposed excitation is defined as follows:

$$f(x) = \begin{cases} \frac{x}{10} & \text{if } 0 \leq x \leq 10 \\ 2 - \frac{x}{10} & \text{if } 10 \leq x \leq 20 \end{cases}$$

To solve this example problem, we applied the method of separation of variables and use Fourier series to expand $f(x)$ into a sum of sine functions. We then solve for the coefficients using the given boundary and initial conditions.

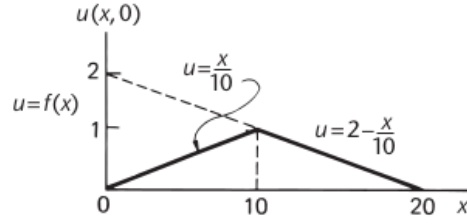


Figure 1: The analytical problem. *Source:* Stroud and Booth (2007)

2.1 Analytical Solution

Implementing the theoretical solution, the eigenvalues and eigenfunctions were obtained in (25) and (26), where P_n and Q_n represent the coefficients for initial displacement and initial velocity, such that $P = B * C$ and $Q = B * D$.

$$\text{Eigenvalues: } \lambda_n = \frac{n\pi}{20} \quad (25)$$

$$\text{Eigenfunctions: } u_n(x, t) = \sin \frac{n\pi x}{20} \left(P_n \cos \frac{n\pi t}{20} + Q_n \sin \frac{n\pi t}{20} \right) \quad (26)$$

Applying initial condition $u(x, 0) = f(x)$ results in (27) since $\sin(0) = 0$ and $\cos(0) = 1$

$$u_n(x, 0) = f(x) = \sum_{n=1}^{\infty} P_n \sin \left(\frac{n\pi x}{20} \right) \quad (27)$$

To determine P_n from $f(x)$ in (27), we apply Fourier techniques and integrate by parts since we have dissimilar functions. The complete integral for P_n is shown in (28), (29)

$$P_n = \frac{2}{20} \int_0^{20} f(x_1) \cdot \sin \left(\frac{n\pi x}{20} \right) + \frac{2}{20} \int_0^{20} f(x_2) \cdot \sin \left(\frac{n\pi x}{20} \right) dx \quad (28)$$

$$10P_n = \int_0^{10} \frac{x}{10} \cdot \sin \left(\frac{n\pi x}{20} \right) dx + \int_{10}^{20} \frac{20-x}{10} \cdot \sin \left(\frac{n\pi x}{20} \right) dx \quad (29)$$

Using integration by parts to solve for $f(x_1)$, we have:

$$u = \frac{x}{10} \Rightarrow du = \frac{1}{10} dx, \quad dv = \sin \left(\frac{n\pi x}{20} \right) dx \Rightarrow v = -\frac{20}{n\pi} \cos \left(\frac{n\pi x}{20} \right)$$

$$f(x_1) = uv - \int v du = \left[\frac{x}{10} \cdot -\frac{20}{n\pi} \cos \left(\frac{n\pi x}{20} \right) \right]_0^{10} - \int_0^{10} -\frac{20}{n\pi} \cos \left(\frac{n\pi x}{20} \right) \cdot \frac{1}{10} dx$$

$$\begin{aligned} f(x_1) : uv &= \frac{10}{10} \cdot \left(-\frac{20}{n\pi} \right) \cos \left(\frac{n\pi \cdot 10}{20} \right) - \frac{0}{10} \cdot \left(-\frac{20}{n\pi} \right) \cos \left(\frac{n\pi \cdot 0}{20} \right) \\ &= -\frac{20}{n\pi} \cos \left(\frac{n\pi}{2} \right) - 0 = -\frac{20}{n\pi} \cos \left(\frac{n\pi}{2} \right) \end{aligned}$$

$$f(x_1) : vdu = - \int_0^{10} \left(-\frac{20}{n\pi} \right) \cos \left(\frac{n\pi x}{20} \right) \cdot \frac{1}{10} dx = \frac{2}{n\pi} \int_0^{10} \cos \left(\frac{n\pi x}{20} \right) dx$$

$$\begin{aligned}
 &= \frac{2}{n\pi} \cdot \frac{20}{n\pi} \left[\sin\left(\frac{n\pi x}{20}\right) \right]_0^{10} = \frac{2}{n\pi} \cdot \frac{20}{n\pi} \left[\sin\left(\frac{n\pi}{2}\right) - \sin(0) \right] = \frac{40}{n^2\pi^2} \sin\left(\frac{n\pi}{2}\right) \\
 f(x_1) &= -\frac{20}{n\pi} \cos\left(\frac{n\pi}{2}\right) + \frac{40}{n^2\pi^2} \sin\left(\frac{n\pi}{2}\right) \tag{30}
 \end{aligned}$$

For $f(x_2)$, we have:

$$f(x_2) = uv - \int v \, du = \left[\frac{20-x}{10} \cdot -\frac{20}{n\pi} \cos\left(\frac{n\pi x}{20}\right) \right]_{10}^{20} + \frac{2}{n\pi} \int_{10}^{20} \cos\left(\frac{n\pi x}{20}\right) dx$$

where:

$$u = \frac{20-x}{10} \Rightarrow du = \frac{1}{10} dx, \quad dv = \sin\left(\frac{n\pi x}{20}\right) dx \Rightarrow v = -\frac{20}{n\pi} \cos\left(\frac{n\pi x}{20}\right)$$

$$\begin{aligned}
 f(x_2) : uv &= \left(\frac{20-20}{10} \cdot -\frac{20}{n\pi} \cos\left(\frac{n\pi \cdot 20}{20}\right) \right) - \left(\frac{20-10}{10} \cdot -\frac{20}{n\pi} \cos\left(\frac{n\pi \cdot 10}{20}\right) \right) \\
 &= 0 - \left(-\frac{20}{n\pi} \cos\left(\frac{n\pi}{2}\right) \right) = \frac{20}{n\pi} \cos\left(\frac{n\pi}{2}\right) \\
 f(x_2) &= \frac{2}{n\pi} \int_{10}^{20} \cos\left(\frac{n\pi x}{20}\right) dx = \frac{2}{n\pi} \left[\frac{20}{n\pi} \sin\left(\frac{n\pi x}{20}\right) \right]_{10}^{20} \\
 &= \frac{2}{n\pi} \left(\frac{20}{n\pi} \sin\left(\frac{n\pi \cdot 20}{20}\right) - \frac{20}{n\pi} \sin\left(\frac{n\pi \cdot 10}{20}\right) \right) \\
 &= \frac{40}{n^2\pi^2} \left(\sin(n\pi) - \sin\left(\frac{n\pi}{2}\right) \right) \\
 &= \frac{40}{n^2\pi^2} \left(2 \sin\left(\frac{n\pi}{2}\right) - \sin\left(\frac{n\pi}{2}\right) \right) \\
 f(x_2) &= \frac{20}{n\pi} \cos\left(\frac{n\pi}{2}\right) + \frac{40}{n^2\pi^2} \left(2 \cdot \sin\left(\frac{n\pi}{2}\right) - \sin\left(\frac{n\pi}{2}\right) \right) \tag{31}
 \end{aligned}$$

Therefore, for $n = 1, 2, 3, \dots$, the complete solution for $10P_n = f(x_1) + f(x_2)$ is:

$$\begin{aligned}
 &= \left[-\frac{20}{n\pi} \cos\left(\frac{n\pi}{2}\right) + \frac{40}{n^2\pi^2} \sin\left(\frac{n\pi}{2}\right) \right] + \left[\frac{20}{n\pi} \cos\left(\frac{n\pi}{2}\right) + \frac{40}{n^2\pi^2} \left(2 \cdot \sin\left(\frac{n\pi}{2}\right) - \sin\left(\frac{n\pi}{2}\right) \right) \right] \\
 10P_n &= \frac{40}{n^2\pi^2} \left(2 \cdot \sin\left(\frac{n\pi}{2}\right) \right) \\
 P_n &= \frac{40}{n^2\pi^2} \left(2 \cdot \sin\left(\frac{n\pi}{2}\right) \right) \cdot \frac{1}{10}
 \end{aligned}$$

$$P_n = \frac{8}{\pi^2 r^2} \sin \frac{r\pi}{2} \quad (32)$$

Substituting equation P_n from (32) in (26), $u(x, t)$ becomes:

$$u_n(x, t) = \sin \frac{n\pi x}{20} \left(\frac{8}{\pi^2 r^2} \sin \frac{r\pi}{2} \cos \frac{n\pi t}{20} + Q_n \sin \frac{n\pi t}{20} \right) \quad (33)$$

Also, at $\frac{\partial u}{\partial t} \Big|_{t=0}$, we have:

$$\frac{\partial u_n}{\partial t} = \sin \frac{n\pi x}{20} \left(\frac{8}{\pi^2 r^2} \sin \frac{r\pi}{2} \left(-\frac{n\pi}{20} \right) \sin \frac{n\pi t}{20} + Q_n \frac{n\pi}{20} \cos \frac{n\pi t}{20} \right)$$

Substituting $t = 0$ into the expression:

$$\frac{\partial u_n}{\partial t} \Big|_{t=0} = \sin \frac{n\pi x}{20} \left(\frac{8}{\pi^2 r^2} \sin \frac{r\pi}{2} \left(-\frac{n\pi}{20} \right) \sin 0 + Q_n \frac{n\pi}{20} \cos 0 \right)$$

Simplifying further:

$$\frac{\partial u_n}{\partial t} \Big|_{t=0} = \sin \frac{n\pi x}{20} \left(0 + Q_n \frac{n\pi}{20} \cdot 1 \right) = \frac{n\pi}{20} Q_n \sin \frac{n\pi x}{20}$$

Now, to show that $Q_r = 0$, we set $\frac{\partial u_n}{\partial t} \Big|_{t=0} = 0$:

$$0 = \frac{n\pi}{20} Q_n \sin \frac{n\pi x}{20}$$

For this equation to hold for **all** x (assuming n and π are nonzero constants), we must have $Q_n = 0$, and therefore, $Q_r = 0$. Note, when $n = 20$, the equation becomes:

$$0 = \pi Q_{20} \sin(\pi x)$$

The sine function, $\sin(\pi x)$, is a periodic function with values ranging between -1 and 1. The only way for the product of πQ_{20} and $\sin(\pi x)$ to be equal to zero is if πQ_{20} is equal to zero as $\sin(\pi x) = 0$ alone, when $\pi Q_{20} > 0$, exist only at the point $y = 0$ on the x-axis. Therefore, the entire equation simplifies to $0 = 0 \times \sin(\pi x)$, which is indeed true for any value of x . Thus, the final solution becomes:

$$u(x, t) = \frac{8}{\pi^2} \sum_{n=1}^{\infty} \frac{1}{r^2} \sin \left(\frac{r\pi x}{20} \right) \sin \frac{r\pi}{2} \cos \frac{r\pi t}{20} \quad (34)$$

The significance of $Q_{20} = 0$ in this context was discussed as it implies that the term associated with $n = 20$ in the Fourier series solution for the wave equation is zero. This means the solution can be accurately represented without the need for a term associated with $n = 20$.

3 Numerical Implementation

To convert the analytical solution into a numerical form, we employed the finite difference method, which is a widely used technique for solving partial differential equations. We discretised both the spatial and temporal domains to approximate the solution. For the spatial domain, we divided the steel structure into a set of discrete spatial points, creating a uniform grid with a spatial resolution denoted as N_x . The spatial step size was calculated as $\Delta x = \frac{L}{N_x}$. Similarly, for the temporal domain, we discretised time into discrete time steps with a temporal resolution represented as N_t , and the time step size was calculated as $\Delta t = \frac{T}{N_t}$ for the analytical solution in (34).

We initialised a 2D array u with dimensions (N_x, N_t) to store the values of displacement at each spatial point and time step. The initial condition $u(x, 0)$ was set based on the $f(x)$ profile. We implemented the central difference scheme to update the values of u at each time step. This scheme approximated the second-order spatial and temporal derivatives and iterated over time steps and spatial points. To visualise the results, we created plots of the displacement u at different time steps. These plots allow us to observe the propagation of waves and different modes in the steel structure.

4 Results and Discussion

Figure 2 illustrates the numerical simulation of the wave equation for different time steps. To validate the effectiveness of the numerical method we consider comparing the numerical output with the results of our analytical solution obtained in equations (32) and (34), shown at a single reference point in Figure (3).

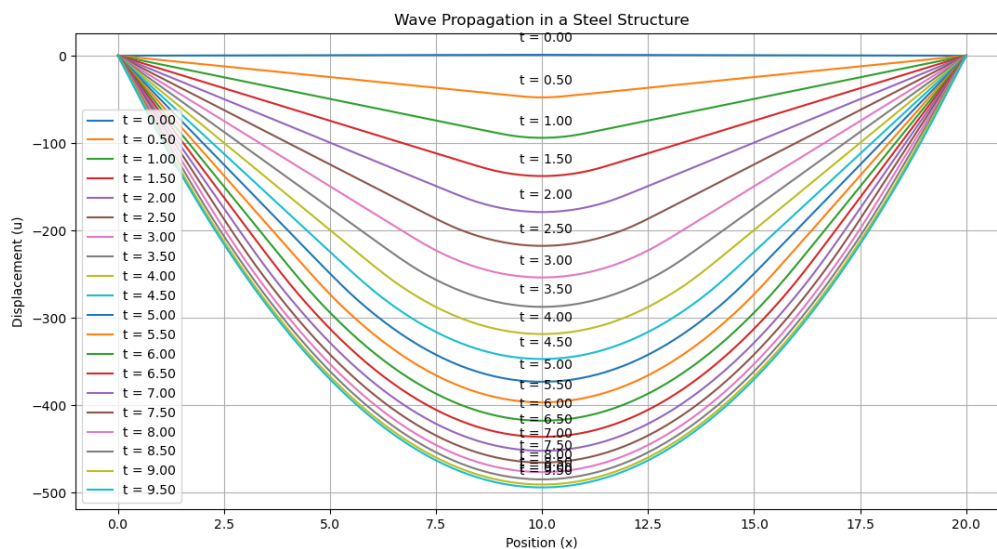


Figure 2: Numerical simulations illustrating the evolution of wave patterns.

To further understand and verify our results, the wave propagation, with a particular focus on the impact of different time step sizes (Δt), was studied. The results were recorded in Table (1). The objective was to obtain agreement between the analytical and numerical solutions, ensuring that the shape of the curves aligns with the problem

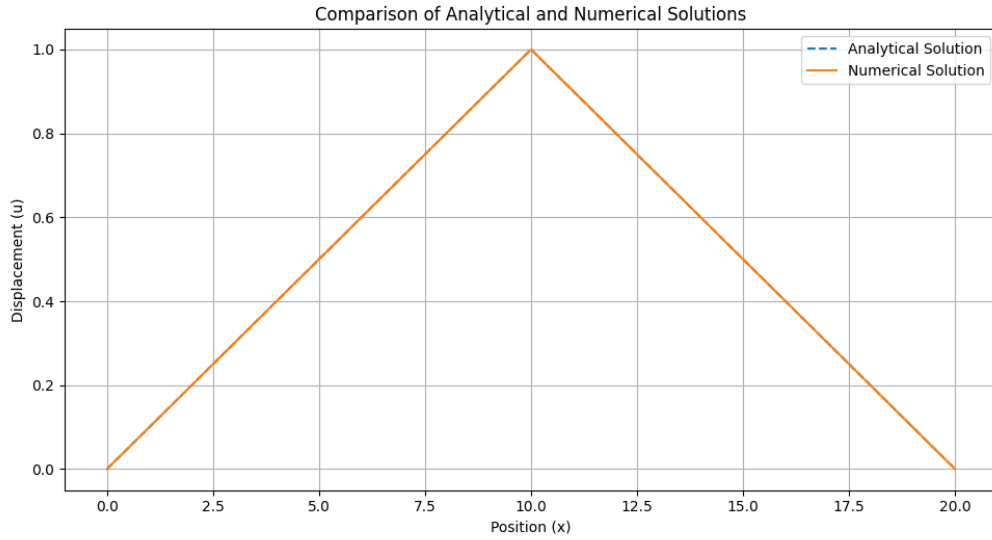


Figure 3: Step size = 3, x-location=5.

Table 1: Comparison of Analytical and Numerical Solutions at $x = 10$, $t = 5$ for Different Δt Values

Δt	Analytical Solution	Numerical Solution
1	3.7525649177131846	5.9939659838946815
2	3.7525649177131846	2.9969841893093094
3	3.7525649177131846	1.9979907907907908
4	3.7525649177131846	1.9979851851851853
5	3.7525649177131846	1.997977977977978
6	3.7525649177131846	0.998998998998999

at hand. The analytical solution served as a reference to which we could compare our numerical results. It was based on a series of terms (P_n) and a double summation to provided an exact representation of the wave propagation in the steel structure even at varying time steps as shown in Figures 4.

To achieve agreement between the analytical and numerical solutions, we implemented a central difference scheme. The finite difference scheme was applied to discretise the partial differential equation governing wave propagation. Our approach was to incrementally vary the time step size (Δt) while keeping other parameters constant.

4.1 Impact of Δt on Results

One of the key observations was that different Δt values indeed yielded different results when compared. As we increased Δt , we noticed a significant impact on the numerical solution. Specifically, larger Δt values led to better alignment of the curves in the analytical and numerical solutions. In contrast, smaller Δt values produced plot results with a higher amplitude for the numerical solution than that of the analytical solution.

We observed that while the amplitude of the curves in the numerical solutions varied with different Δt values, the shape of the curves consistently adhered to the prescribed

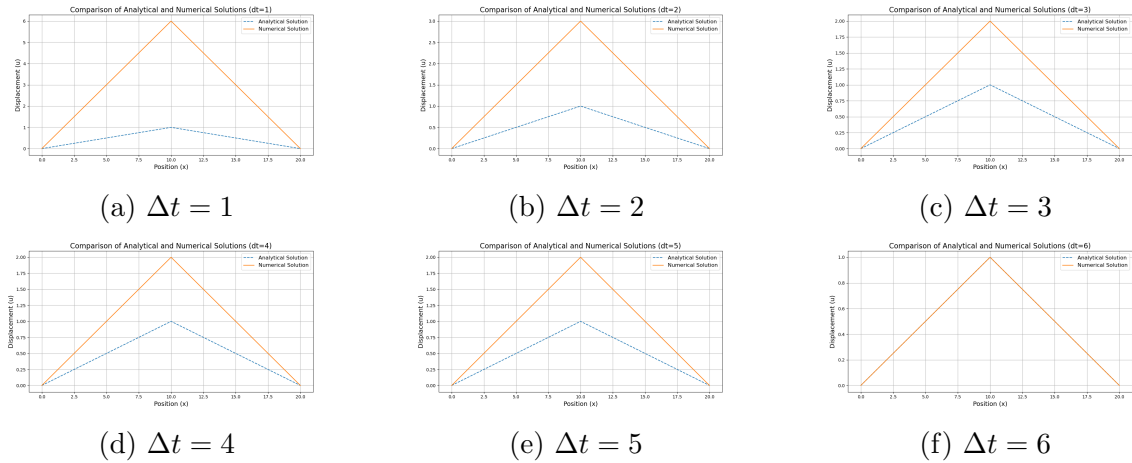


Figure 4: Comparison of Analytical and Numerical Solutions at $x = 10, t = 5$ for Different Δt Values

boundary conditions. This is a vital finding, as it implies that the fundamental physics of wave propagation in the steel structure remained intact. Despite variations in amplitude, the waveforms exhibited the expected behavior in terms of their spatial and temporal evolution.

In Figure 3, we visually demonstrated the agreement between the analytical and numerical solutions at a specific spatial position ($x = 10$) and time ($t = 5$) in line with previous discussion. Varying the Δt values from 1 to 6 help us captured the changing behavior of the numerical solution. It is evident that larger Δt values, as seen in Figure (4) *f*, provided results that closely matched the analytical solution perfectly, both in terms of shape and amplitude. As Δt decreased, however, the amplitude of the numerical solution exhibited larger deviations from the analytical curve, but maintained expected shape of the curve function.

This underscores the significance of careful consideration when selecting time step sizes in numerical simulations. While larger time steps may offer computational advantages, they can lead to inaccuracies in capturing the physics of the problem. Future work may involve a more thorough exploration of the numerical stability and convergence properties of the chosen finite difference scheme. This would provide better insights into the variation in amplitudes we experienced while we varied the temporal resolution.

5 Conclusion

Our work underscores the significance of achieving not only agreement between analytical and numerical solutions but also maintaining consistency in modeling physical behavior. Through the examination of different Δt values, we have illustrated the trade-offs between computational efficiency and solution accuracy in the context of wave propagation. It emphasises the critical intersection of theoretical principles and practical applications within the realm of engineering mathematics, with a primary focus on enhancing the educational experience for students. In this context, we offer several noteworthy contributions:

1. We have effectively demonstrated the relationship between theoretical derivations and their practical applications, bridging the gap between abstract mathematical

concepts and real-world scenarios.

2. The utilisation of Fourier series techniques in solving the classical wave equation, coupled with boundary and initial conditions and integration by parts, has been showcased as a powerful tool in engineering mathematics.
3. Our work has successfully implemented both analytical and numerical methods to unravel intricate problems in engineering, providing students with valuable problem-solving skills.
4. Through numerical simulations, we highlight the practical effectiveness of theoretical concepts in addressing complex engineering challenges. This approach offers students a tangible understanding of theoretical principles in action.

References

1. K. A. Stroud and Dexter J. Booth. (2007). *Engineering Mathematics* (6th ed.). Macmillan International Higher Education. ISBN: 978-1-4039-4454-9.
2. Yang, Xiao-jun, Abdulrahman Alsolami, and Ahmed Ali. (2023). An even entire function of order one is a special solution for a classical wave equation in one-dimensional space. *Thermal Science*.
3. Wang, Xueting, Min Lin, Jian Li, Junkai Tong, Xinjing Huang, Lin Liang, Zheng Fan, and Yang Liu. (2022). Ultrasonic guided wave imaging with deep learning: Applications in corrosion mapping. *Mechanical Systems and Signal Processing*.
4. Walker, B. J., A. Townsend, Alexander K. Chudasama, and Andrew L. Krause. (2023). VisualPDE: rapid interactive simulations of partial differential equations.
5. Nagarajaiah, Satish. (2021). Data-Driven Theory-Guided Learning of Partial Differential Equations Using Simultaneous Basis Function.
6. Ding, Wei, John P. Hollkamp, Sansit Patnaik, and Fabio Semperlotti. (2022). On the fractional homogenization of one-dimensional elastic metamaterials with viscoelastic foundation. *Archive of Applied Mechanics*.
7. Chen, Jiaji, Yangyang Chen, Xianchen Xu, Weijian Zhou, and Guoliang Huang. (2022). A physics-guided machine learning for multifunctional wave control in active metabeams. *Extreme Mechanics Letters*.
8. Prieur, Christophe, Sophie Tarbouriech, J.M. Gomes da Silva, and João Manoel Gomes da Silva. (2014). Well-posedness and stability of a 1D wave equation with saturating distributed input. *IEEE Conference on Decision and Control*.
9. Lomovtsev, F. E., and K. A. Spesivtseva. (2021). Mixed problem for a general 1D wave equation with characteristic second derivatives in a nonstationary boundary mode. *Mathematical Notes*.
10. Guo, Wei, Hua-cheng Zhou, and Miroslav Krstic. (2018). Adaptive error feedback regulation problem for 1D wave equation. *International Journal of Robust and Nonlinear Control*.
11. Ye, H., Liang, B., Ng, OL., et al. (2023). Integration of computational thinking in K-12 mathematics education: a systematic review on CT-based mathematics

instruction and student learning. *IJ STEM Ed*, 10(3).

<https://doi.org/10.1186/s40594-023-00396-w>

12. Teaching Mathematics and its Applications: An International Journal of the IMA, Volume 42, Issue 2, June 2023, Pages 126–149.
<https://doi.org/10.1093/teamat/hrac005>.
13. Faezeh Rezvanifard, Farzad Radmehr, Yuriy Rogovchenko. (2023). Advancing engineering students' conceptual understanding through puzzle-based learning: a case study with exact differential equations. *Teaching Mathematics and its Applications: An International Journal of the IMA*, 42(2), 126–149.
<https://doi.org/10.1093/teamat/hrac005>.

Appendix 1

To show the equation in (16) holds, we apply the identity $\sin^2(\theta) = \frac{1}{2} - \frac{1}{2} \cos(2\theta)$.

$$\begin{aligned}
 \int_0^L B_m \sin^2\left(\frac{m\pi x}{L}\right) dx &= \frac{L}{2} B_m \\
 \int_0^L B_m \sin^2\left(\frac{m\pi x}{L}\right) dx &= \int_0^L B_m \left(\frac{1}{2} - \frac{1}{2} \cos\left(\frac{2m\pi x}{L}\right)\right) dx \\
 &= \frac{B_m}{2} \int_0^L \left(1 - \cos\left(\frac{2m\pi x}{L}\right)\right) dx \\
 &= \frac{B_m}{2} \left[x - \frac{L}{2m\pi} \sin\left(\frac{2m\pi x}{L}\right) \right]_0^L \\
 &= \frac{B_m}{2} \int_0^L (1 - \cos\left(\frac{2m\pi x}{L}\right)) dx \\
 &= \frac{B_m}{2} \left[x - \frac{L}{2m\pi} \sin\left(\frac{2m\pi x}{L}\right) \right]_0^L \\
 &= \frac{B_m}{2} \left[L - \frac{L}{2m\pi} \sin\left(\frac{2m\pi L}{L}\right) - 0 + \frac{L}{2m\pi} \sin\left(\frac{2m\pi \cdot 0}{L}\right) \right] \\
 &= \frac{B_m}{2} \left[L - \frac{L}{2m\pi} \sin(2m\pi) + \frac{L}{2m\pi} \sin(0) \right] \\
 &= \frac{B_m}{2} \left[L - \frac{L}{2m\pi} \cdot 0 + \frac{L}{2m\pi} \cdot 0 \right] \\
 &= \frac{L}{2} B_m
 \end{aligned}$$

Appendix 2

Algorithm 1 Numerical Implementation Pseudocode

```

1: Initialisation:
2: Define constants:
3:  $L$ : Length of the steel structure
4:  $Nx$ : Number of spatial points
5:  $Nt$ : Number of time steps
6:  $dt$ : Temporal step size
7: Create a 2D array  $u$  with dimensions  $(Nx, Nt)$  to store displacements
8: Set Initial Condition:
9: Initialise the spatial domain  $x = [0, L]$  with  $Nx$  points
10: Set  $u(x, 0)$  based on the initial displacement profile  $f(x)$ 
11: Numerical Scheme (Finite Difference):
12: for  $n$  from 1 to  $Nt - 1$  do
13:   for  $i$  from 1 to  $Nx - 1$  do
14:     Update  $u(i, n + 1)$  using the central difference scheme:
15:     
$$u(i, n + 1) = 2 \cdot u(i, n) - u(i, n - 1) + (dt^2) \cdot \left(\frac{dx^2}{L^2}\right) \cdot (u(i + 1, n) - 2 \cdot u(i, n) + u(i - 1, n))$$

16:   end for
17: end for
18: Visualisation:
19: Create plots to visualise the wave propagation:
20: for selected time steps (e.g., every 50 time steps) do
21:   Plot  $u(x, t)$  for the current time step
22:   Add an annotation with the corresponding time value
23: end for
24: Display the plots to visualise the wave evolution

```

Python Code:

```

def analytical_f(x): # Define the analytical solution for f(x)
    return np.piecewise(x, [x < 10, x >= 10], [lambda x: x / 10, lambda x: (20 - x) / 10])

def calculate_coefficient_Pn(n): # Define a function to calculate P_n
    L = 20.0 # Length of the steel structure
    r = (n * np.pi) / L
    Pn = (8 / (np.pi ** 2 * r ** 2)) * np.sin(r * np.pi / 2)
    return Pn

def calculate_u(x, t, max_n): # Define a function to calculate u(x, t) based on coefficients P_n
    u = 0
    for n in range(1, max_n + 1):
        Pn = calculate_coefficient_Pn(n)
        u += Pn * np.sin(n * np.pi * x / 20) * np.sin(n * np.pi / 2) * np.cos(n * np.pi * t / 20)
    return u

# Simulate the numerical solution (central difference scheme)
L = 20.0
Nx = 1000
dx = L / Nx
x_values = np.linspace(0, L, Nx)
Nt = 1000
dt = 1
t_values = np.linspace(0, 10, Nt)
numerical_results = np.zeros((Nx, Nt))

numerical_results[:, 0] = analytical_f(x_values) # Initialize numerical solution at t=0

for n in range(Nt - 1):
    for i in range(1, Nx - 1):
        numerical_results[i, n + 1] = 2 * numerical_results[i, n] - numerical_results[i, n - 1] + \
            (dt**2) * (dx**2) * (numerical_results[i + 1, n] - 2 * numerical_results[i, n] + numerical_results[i - 1, n])

x_compare = 10 # Example position to compare # Comparison at specific positions and times
t_compare = 5 # Example time to compare
max_n = 10 # Increased max_n for more terms

analytical_value = calculate_u(x_compare, t_compare, max_n)
numerical_value = numerical_results[int(x_compare / dx), int(t_compare / dt)]

```